

# Desalination of brines by membrane distillation

L. Martínez-Díez\*, F.J. Florido-Díaz

*Department of Applied Physics, Faculty of Science, University of Málaga, 29071 Málaga, Spain  
Tel. +34 (95) 213-1924; Fax +34 (95) 213-2000; email: lmartinez@uma.es*

Received 24 July 2000; accepted 14 August 2000

---

## Abstract

Membrane distillation (MD) has been used for water production from brines at temperatures below 50°C. The effect of recirculation rate, mean temperature and salt concentration on the water fluxes has been measured. The experiments have been carried out with a commercial composite membrane formed by an actual porous PTFE top layer on a PP screen support. Experimental flux results vs. salt concentration have been fitted to the MD classical heat transfer model correlations, envisaging the membrane support as an additional heat transfer resistance in the liquid form. In this way we have obtained the value of unknown parameters of the model. This allows for predictions on the MD performance of the studied membrane for experimental conditions different of those considered in this work. The membrane permeability coefficient obtained from the above-mentioned fits is in good accordance with that predicted by a Knudsen mechanism to model the vapour transport across the membrane.

*Keywords:* Membrane distillation; Hydrophobic membrane; Knudsen diffusion; Heat transport

---

## 1. Introduction

Membrane distillation (MD) is a membrane technique that involves transport of water vapour through the pores of hydrophobic membranes due to a vapour pressure driving force provided by temperature and/or solute concentration differences across a membrane. A variety of methods may be employed to impose this vapour pressure

difference. In the present work the direct contact membrane distillation method is considered. In this configuration the surfaces of the membrane are in direct contact with two liquid phases, the feed (warm solution) and the permeate (cold solution), kept at different temperatures. A liquid vapour interface exists at the pore entrances where liquid–vapour equilibrium is established. Inside the pores only a gaseous phase is present through which vapour is transported as long as a partial pressure difference is maintained. The

---

\*Corresponding author.

*Presented at the conference on Desalination Strategies in South Mediterranean Countries, Cooperation between Mediterranean Countries of Europe and the Southern Rim of the Mediterranean, sponsored by the European Desalination Society and Ecole Nationale d'Ingenieurs de Tunis, September 11–13, 2000, Jerba, Tunisia.*

vaporization takes place at the feed membrane interface. The vapour flows through the membrane pores and condenses at the permeate membrane interface. Thus the separation mechanism of membrane distillation is based on a vapour–liquid equilibrium.

The main advantage of membrane distillation over the traditional distillation process is associated with the possibility of working at low temperatures and/or using low-grade, waste or alternative energy sources. In the present work MD is used for water production from brines at temperatures below 50°C. The experimental water flux results have been fitted to a model which is based on the temperature polarization effects and on the mechanisms of heat and mass transfer. The composite membrane is split into a series of two heat transfer resistances associated to the top layer (dry) and the support layer (wetted), respectively. The membrane permeability coefficient has been obtained from the analysis of the results according to the model, and the value obtained suggest a mechanism based largely on the Knudsen diffusion for the transmembrane water vapour transport.

## 2. Experimental

A flat sheet commercial membrane, TF200, supplied by Gelman Instruments, was used. This membrane is made of a thin polytetrafluoroethylene (PTFE) porous layer, supported by a polypropylene (PP) net. The principal structural characteristics as specified by the manufacturers are: 0.20 µm nominal pore diameter, 178 µm thickness and 80% porosity. The membrane was observed by scanning electron microscopy showing pores of various sizes. From measurements [1] of air–liquid displacement porosimetry, the pore geometry factor and mean pore radius were measured as  $\varepsilon/\chi\delta = 5130\text{m}^{-1}$  and  $r = 0.16\text{ }\mu\text{m}$ , respectively. The PP net has hole sizes greater than 500 µm and a thickness of 120 µm.

The thickness of the PTFE layer is 60 µm. In all the experiments the PP support was in direct contact with the permeate.

The salt solutions were prepared by dissolving pure pro-analysis grade sodium chloride with bi-distilled pure water.

The MD measurements were carried [2] out using a membrane module composed of two symmetrical compartments between which the flat-sheet membrane was sandwiched. Each compartment is made of nine channels — each 55 mm long, 7 mm wide and 0.4 mm high. In all experimental runs the membrane was maintained in a horizontal position. The feed solution was preheated in a thermostated bath and then pumped onto the lower membrane surface. Water was likewise preheated (at a lower temperature than the feed solution) in another thermostated bath and then pumped onto the upper membrane surface. All liquids were suitably degassed beforehand in order to avoid bubble formation. The recirculation of the fluids on both sides of the membrane was in countercurrent directions. Flow rates were maintained approximately equal for both streams. The temperatures of the bulk liquid phases were measured at the hot entrance,  $T_{b1-in}$ , the cold entrance,  $T_{b2-in}$ , the hot exit,  $T_{b1-out}$ , and the cold exit,  $T_{b2-out}$ , of the membrane cell. In the following study the mean values,

$$T_{b1} = \frac{T_{b1-in} + T_{b1-out}}{2} \quad (1)$$

$$T_{b2} = \frac{T_{b2-in} + T_{b2-out}}{2} \quad (2)$$

will be considered as bulk temperatures of distillate and feed and distillate permeate, respectively. In the experimental set-up the permeate continuously flows out of the distillate reservoir, and the corresponding distillate flux was measured by collecting this liquid flowing out of the cold reservoir.

Different experiments were carried out using feed solutions of concentrations 0, 0.55, 1.15 and 1.65 molar. In all cases, from the beginning of the runs, pure water was recirculated in the cold semi-cell. For each feed solution, three different series of experiments were conducted at temperatures  $T_{b1}$  of 25, 35 and 45°C and temperatures  $T_{b2}$  of 15, 25 and 35°C, respectively. In each case the mass fluxes for recirculation flow rates of 7, 11 and 15 cm<sup>3</sup>/s were measured.

### 3. Theory

The system to be studied consists of a porous hydrophobic membrane that separates two aqueous phases maintained at different temperatures and concentrations. The basic equation used to describe the transmembrane water vapour flux in membrane distillation is Eq. (3), which relates the mass flux,  $J$ , to the driving force represented by the vapour pressure difference between both liquid–vapour interfaces of the membrane ( $p_{m1}-p_{m2}$ ) via a proportionality coefficient,  $C$ , which is considered as the membrane permeability coefficient,

$$J = C(p_{m1} - p_{m2}) \quad (3)$$

The driving force depends on the temperature as well as the solute concentration values prevailing at the vapour–liquid interfaces. As such interface values are of different bulk values and not accessible, another representation of mass transport is given by Eq. (4), which refers to the bulk conditions of the liquid compartments:

$$J = A(T_{b1} - T_{b2}) - B(x_{b1} - x_{b2}) \quad (4)$$

where  $x$  is the mole fraction of dissolved species. Expressions for the phenomenological coefficients  $A$  and  $B$  may be obtained [3] as indicated below.

The driving force for water transport may be written:

$$\begin{aligned} p_{m1} - p_{m2} &= p_{m1}^* x_{w1} \gamma_{w1} - p_{m2}^* x_{w2} \gamma_{w2} \\ &= (p_{m1}^* - p_{m2}^*)(1 - \bar{x}) - \bar{p}_m^* (x_1 - x_2) \end{aligned} \quad (5)$$

where the upper index “\*” means pure water at the same temperature,  $\gamma_w$  is the activity coefficient,  $x_w$  the water mole fraction and  $x$  the total ionic mole fraction. The line over a magnitude means average value of this magnitude in the membrane. Eq. (5) is a good approximation for  $(p_{m1}-p_{m2})$  when the salt concentration is lower than 2 molar.

On the other hand, by using the Clausius–Clapeyron equation, the temperature difference across the membrane ( $T_{m1}-T_{m2}$ ) may be related with the difference  $(p_{m1}^*-p_{m2}^*)$  if the first is relatively small, in the form:

$$p_{m1}^* - p_{m2}^* = \left( \frac{p_m^* \Delta H_v M}{RT^2} \right) (T_{m1} - T_{m2}) \quad (6)$$

with the first parenthesis evaluated at the mean temperature in the membrane, and where  $\Delta H_v$  is the latent heat of vaporization,  $M$  the molecular weight of water and  $R$  the gas constant.

Standard steady-state heat transfer considerations across the various elements (feed thermal boundary layer, porous membrane, net and permeate thermal boundary layer) of the membrane system allow to write

$$\begin{aligned} Q &= h_1(T_{b1} - T_{m1}) = J \Delta H_v + h_m(T_{m1} - T_{m2}) \\ &= \left( \frac{1}{h_{net}} + \frac{1}{h_2} \right)^{-1} (T_{m2} - T_{b2}) = h_{net-2} (T_{m2} - T_{b2}) \end{aligned} \quad (7)$$

where  $Q$  is the transmembrane heat flux,  $h_1$  and  $h_2$  represents the heat transfer coefficients of the

feed and permeate thermal boundary layers,  $h_m$  is the heat transfer coefficient of the membrane and  $h_{net}$  is the heat transfer coefficient of the net with the liquid water entrapped. Here we assume, as did Curiel et al. [4], that the porous PTFE layer is the only part of the membrane participating in the water transport in vapour phase, while the PP net contributes to the heat transfer resistance in the liquid form. Eq. (7) allows us to write the temperature polarization coefficient as:

$$\frac{T_{m1} - T_{m2}}{T_{b1} - T_{b2}} = \frac{1 - \frac{1}{h_L} \frac{J \Delta H_v}{(T_{b1} - T_{b2})}}{1 + \frac{h_m}{h_L}} \quad (8)$$

where

$$\frac{1}{h_L} = \frac{1}{h_1} + \frac{1}{h_{net}} + \frac{1}{h_2} \quad (9)$$

Likewise Eq. (7) allows us to write the difference between the mean membrane temperature and the mean bulk temperature as:

$$\bar{T}_m - \bar{T}_b = (T_{b1} - T_{b2}) \left( 1 - \frac{T_{m1} - T_{m2}}{T_{b1} - T_{b2}} \right) \frac{h_1 - h_{net-2}}{h_1 + h_{net-2}} \quad (10)$$

Having in mind Eqs. (5), (6) and (8), Eq. (3) may be written:

$$J = \frac{K_D}{1 + K_T K_D \frac{\Delta H_v}{h_L}} \left[ K_T (T_{b1} - T_{b2}) - (x_{m1} - x_{m2}) \right] \quad (11)$$

where

$$K_D = C \bar{P}_m^* \quad (12)$$

and

$$K_T = (1 - \bar{x}) \frac{\Delta H_v M h_L}{R \bar{T}^2 (h_m + h_L)} \quad (13)$$

In a previous paper [5] we have shown that the concentration polarization is insignificant, resulting in  $x_{m1} = x_{b1}$ . In this way the comparison of Eqs. (11) and (4) will give us the calculation of coefficient  $C$  if we previously determine coefficients  $A$  and  $B$ .

#### 4. Results and discussion

The experimental results of water flux for different values of temperatures, recirculation rate and concentration are shown in Figs. 1–3. The solid lines are the linear fits of the experimental data corresponding to different mean bulk temperatures,  $(T_{b1} + T_{b2})/2$ . In all the experiments the temperature difference  $(T_{b1} - T_{b2})$  was 10°C. It can be seen from these figures that the water flux increases as the mean temperature in the membrane system increases. The water flux increases in more than 100% when the mean temperature is increased from 20 to 40°C. Figs. 1–3 also show that the flux increases with the recirculation rate. A rough estimation is that the water flux increases to about 10–12% when one compares the values obtained for a recirculation rate of 7 cm<sup>3</sup>/s, and the values obtained for a recirculation rate are 15 cm<sup>3</sup>/s. Finally, Figs. 1–3 show that the flux decreases, in an approximated linear way, with the salt concentration of feed solution. The mentioned trends are in accordance with the model described in the previous section. Thus, we have used the equations of the model in order to obtain important information about the membrane system.

First, the experimental points  $\{x_{b1}; J\}$  have been fitted to a linear function by a least squares

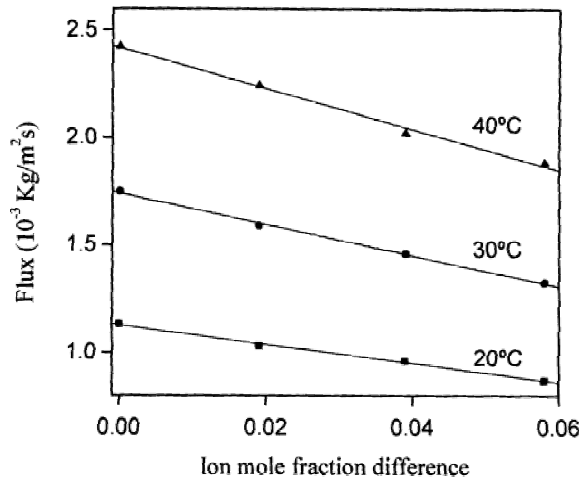


Fig. 1. Mass flux ( $10^{-3}$  kg/m<sup>2</sup>s) vs. ion mole fraction difference for three mean bulk temperatures. The recirculation rate was 7 cm<sup>3</sup>/s.

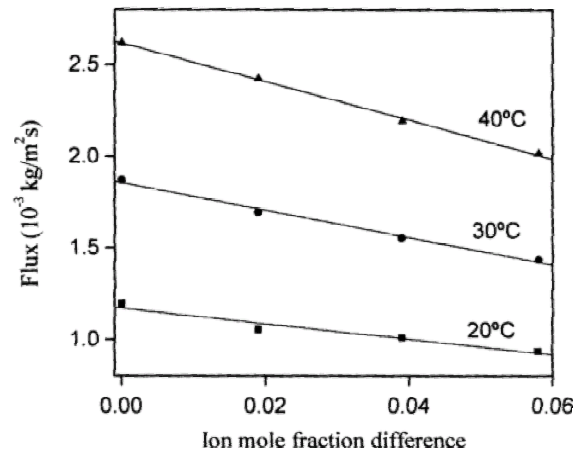


Fig. 2. Mass flux ( $10^{-3}$  kg/m<sup>2</sup>s) vs. ion mole fraction difference for three mean bulk temperatures. The recirculation rate was 11 cm<sup>3</sup>/s.

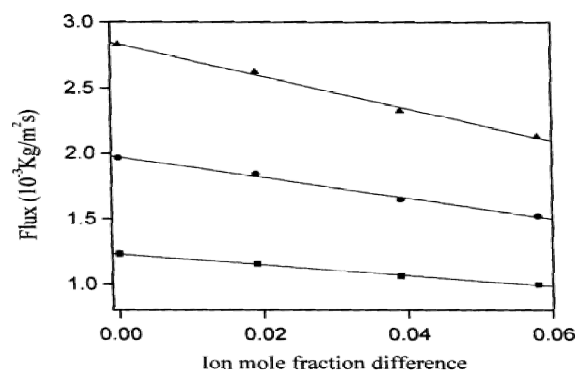


Fig. 3. Mass flux ( $10^{-3}$  kg/m<sup>2</sup>s) vs. ion mole fraction difference for three mean bulk temperatures. The recirculation rate was 15 cm<sup>3</sup>/s.

method. The slope of each one of the straight lines is the value of the corresponding coefficient  $B$  in Eq. (4). The intercept of each one of the lines is the corresponding value of the product  $A(T_{b1}-T_{b2})$ , and the value of the coefficient  $A$  may be obtained. The results are shown in Table 1.

Having in mind Eqs. (4) and (11), the coefficients  $K_T$  and  $K_D$  were calculated from the

corresponding values of  $A$  and  $B$ . Previously we calculated  $h_L$  from Eq. (9), estimating  $h_1$  and  $h_2$  with the help of empirical correlations of dimensionless Nusselt, Reynolds and Prandtl numbers. A value of 2930 W/m<sup>2</sup>K was used for  $h_{net}$  as estimated by Courel et al. [4] for the same membrane.

The heat transfer coefficient of the membrane  $h_m$  can be obtained from the  $K_T$  results using Eq. (13). Values ranging between 1200 and 1300 W/m<sup>2</sup>K were obtained, similar to the value of 1210 W/m<sup>2</sup>K estimated by Courel et al. [4].

In order to be able to calculate coefficient  $C$ , the temperature polarization coefficient and the temperature difference ( $\bar{T}_m - \bar{T}_b$ ) were obtained using Eqs. (8) and (10), respectively. The results are given in Table 1 and indicate an important temperature difference between  $\bar{T}_m$  and  $\bar{T}_b$ , due to the asymmetry of the membrane system. This asymmetry is associated to the membrane support with entrapped liquid water. Finally, this difference is kept in mind in order to obtain the PTFE layer permeability coefficient  $C$  from Eq. (12). Values ranging between 21 and 27 × 10<sup>-7</sup> kg/m<sup>2</sup>sPa were obtained, compatible with the

Table 1

Results of  $A$  and  $B$  coefficients, temperature polarization and difference between mean membrane temperature and mean bulk temperature for different recirculation rates and temperatures

$q$ , cm <sup>3</sup> /s	$\bar{T}_b$ , °C	$A \times 10^4$ , kg/m <sup>2</sup> s K	$B \times 10^3$ , kg/m <sup>2</sup> s	$\frac{T_{m1} - T_{m2}}{T_{b1} - T_{b2}}$	$\bar{T}_m - \bar{T}_b$ , °C
7	20	1.13	4.40	0.31	2.34
7	30	1.74	7.23	0.25	2.57
7	40	2.42	9.52	0.21	2.73
11	20	1.17	4.25	0.34	2.46
11	30	1.86	7.49	0.26	2.77
11	40	2.62	1.06	0.21	3.01
15	20	1.23	4.12	0.37	2.49
15	30	1.97	7.89	0.27	2.93
15	40	2.84	12.46	0.19	3.29

coefficient predicted by the Knudsen diffusion model,

$$C = 1.064r \frac{\varepsilon}{\chi \delta} \left( \frac{M}{RT} \right)^{0.5} \quad (14)$$

if the estimated value of 0.16  $\mu\text{m}$  and 5130  $\text{m}^{-1}$  for  $r$  and  $\varepsilon/\chi\delta$ , respectively, are considered.

The model described and the values obtained for parameters  $h_m$  and  $C$  allow predictions on the performance of the studied membrane for experimental conditions different from those considered in this work.

## 5. Conclusions

1. The effects of temperature, flow rate and feed concentration on permeate flux have been studied for a direct contact type module.

2. The results show qualitative accordance with the model described.

3. The experimental results have been fitted to the model equations and quantitative values of fundamental parameters have been obtained.

## 6. Symbols

$A$	— Phenomenological coefficient defined in Eq. (4), kg/m <sup>2</sup> s K
$B$	— Phenomenological coefficient defined in Eq. (4), kg/m <sup>2</sup> s
$C$	— Membrane coefficient, kg/m <sup>2</sup> s Pa
$\Delta H_v$	— Latent heat of vaporization, J/kg
$h$	— Film heat transfer coefficient, W/m <sup>2</sup> K
$h_L$	— Heat transfer coefficient defined in Eq. (9), W/m <sup>2</sup> K
$h_{\text{net}}$	— Heat transfer coefficient defined in Eq. (7), W/m <sup>2</sup> K
$J$	— Mass flux, kg/m <sup>2</sup> s
$K_D$	— Defined by Eq. (12), kg/m <sup>2</sup> s
$K_T$	— Defined by Eq. (13), K <sup>-1</sup>
$M$	— Molecular weight of water, kg/mol
$p$	— Vapour pressure, Pa
$p^*$	— Vapour pressure of pure water, Pa
$q$	— Recirculation rate, m <sup>3</sup> /s
$Q$	— Heat flux, W/m <sup>2</sup>
$r$	— Pore radius, m
$R$	— Gas constant, J/mol K
$T$	— Temperature, K
$x$	— Mole fraction of dissolved species, dimensionless

*Greek*

- $\delta$  — Membrane thickness, m  
 $\varepsilon$  — Membrane porosity, dimensionless  
 $\chi$  — Pore tortuosity factor, dimensionless

*Subscripts*

- b — Bulk  
m — Membrane  
net — Membrane net with liquid entrapped  
in — Entrance of the membrane module  
out — Exit of the membrane module  
1 — Warm side  
2 — Cold side

**References**

- [1] L. Martínez-Díez and F.J. Florido-Díaz, submitted for publication.  
[2] L. Martínez-Díez and M.I. Vázquez-González, *AIChE J.*, 42(7) (1996) 1844.  
[3] G.C. Sarti and C. Gostoli, in: E. Drioli and M. Nakagaki, eds., *Membranes and Membrane Processes*, Plenum Press, New York, 1986, pp. 349–360.  
[4] M. Curiel, M. Dornier, G. Marcel Rios and M. Reynes, *J. Membr. Sci.*, 173 (2000) 107.  
[5] L. Martínez-Díez and M.I. Vázquez-González, *J. Membr. Sci.*, 156 (1999) 265.